Published in final edited form as:

*Wiley Interdiscip Rev Nanomed Nanobiotechnol*. 2023 ; 15(5): e1911. doi:10.1002/wnan.1911.

# Pumped and Pumpless Microphysiological Systems to Study (Nano)therapeutics

**Eun-Jin Lee**,
University of Maryland and NIST, PML

**Zachary Krassin**,
Binghamton University

**Hasan Erbil Abaci**,
Columbia University Medical Center

**Gretchen J. Mahler**,
Binghamton University

**Mandy B. Esch**
NIST, PML

## Abstract

Fluidic microphysiological systems (MPS) are microfluidic cell culture devices that are designed to mimic the biochemical and biophysical *in vivo* microenvironments of human tissues better than conventional petri dishes or well-plates. MPS-grown tissue cultures can be used for probing new drugs for their potential primary and secondary toxicities as well as their efficacy. The systems can also be used for assessing the effects of environmental nanoparticles and nanotheranostics, including their rate of uptake, biodistribution, elimination, and toxicity. Pumpless MPS are a group of MPS that often utilize gravity to recirculate cell culture medium through their microfluidic networks, providing some advantages, but also presenting some challenges. They can be operated with near-physiological amounts of blood surrogate (i.e. cell culture medium) that can recirculate in bidirectional or unidirectional flow patterns depending on the device configuration. Here we discuss recent advances in the design and use of both pumped and pumpless MPS with a focus on where pumpless devices can contribute to realizing the potential future role of MPS in evaluating nanomaterials.

## Graphical/Visual Abstract and Caption

mandy.esch@nist.gov .

**Conflict of Interest:** There are no conflicts of interest.

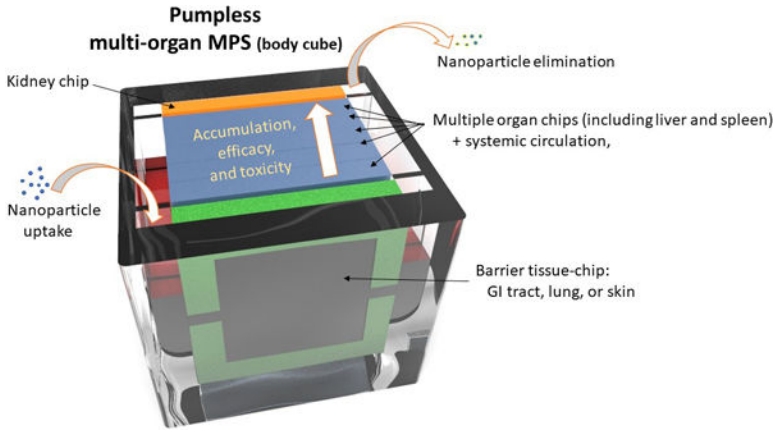


Abstract Figure: Pumpless MPS can be used to estimate the rate of nanoparticle uptake, biodistribution, elimination, and toxicity. Tissue-chip-integrated measurements of tissue health and function can help with estimating the particles' efficacy and/or potential adverse effects.

## 1. Introduction

### 1.1 The Power of fluidic MPS

Fluidic microphysiological systems (MPS) are small devices that contain surfaces or chambers for the growth of human cells under microfluidic flow. The cells cultured on each surface (or in each chamber) represent tissues or even entire organs that are typically $1/100000^{th}$ to $1/50000^{th}$ of the size of the corresponding organ in the human body. MPS can contain more than one organ chamber (multi-organ MPS). The devices also typically include a mechanism to recirculate cell culture medium (blood surrogate) to mimic the circulation of blood.

MPS can be powerful *in vitro* mimics of human organs (or a subset of organs) because the surfaces and chambers can provide microscale biophysical and biochemical cues that help reproduce a cell's (or a tissue's) microenvironment inside the body. For example, lung epithelial cells grown on a membrane that is periodically stretched, experience the mechanical stress that breathing causes in lung tissue (Huh et al., 2010). Endothelial cells grown within microfluidic channels experience the mechanical shear that blood flow causes in some blood vessels (Traore & George, 2017), and liver cells grown in different regions of a microfluidic chip can be exposed to high or low oxygen concentrations, similar to what they would experience in different zones within liver tissue *in vivo* (Y. B. Kang et al., 2020; Y. B. A. Kang et al., 2018). Such microscale conditions provide cues that may influence how the tissue mimics interact with drugs or nanoparticles.

MPS that contain several organ chambers and a mechanism to recirculate cell culture medium (blood surrogate) among organ chambers can identify primary effects stemming from the original drug or nanoparticle challenge, as well as secondary effects stemming from drug metabolites or from the tissues' responses to nanoparticles. To measure secondary effects, any soluble proteins produced by tissues should ideally reach concentrations similar to those found in the circulation of a patient. To achieve that, MPS can be designed to

mimic appropriate blood residence times within a given tissue volume. Equally important is the volume of blood surrogate that recirculates within the device. That volume can be scaled using the same scaling factor that is used for all other tissues in the MPS so that biomarker or drug metabolite concentrations approach levels similar to what they might be in the human body.

Though still under discussion, several reviews have provided a general framework for designing MPS so that data obtained with them can help with choosing suitable drug concentrations for clinical trials (Andersen et al., 2014; Edington et al., 2018; A. S. Smith et al., 2013). Here we discuss advantages and disadvantages of pumpless MPS and how the devices could contribute to assessing nanoparticle therapeutics.

### 1.2 Advantages and disadvantages of pumpless MPS

Pumpless MPS utilize gravity to drive fluid through organ chambers, making both external and system-integrated pumps unnecessary. The lack of pumps simplifies the operation of such devices and often also lessens the generation of air bubbles in the fluidic circuits. The first pumpless microfluidic tissue culture systems were developed for liver tissue where the device was rocked back and forth, and cell culture medium alternated between forward and backward flow across the tissue (Sung, Kam, et al., 2010). Follow-up systems have incorporated many more organ chambers, resulting in pumpless multi-organ MPS (Miller & Shuler, 2016; Oleaga et al., 2016).

To create a pressure drop between two medium reservoirs using gravity, the devices are placed at an angle using a rocker or a rotating platform (Fig. 1). To create physiological flow rates in each organ chamber, either active or passive flow control mechanisms must be integrated. The most commonly used mechanism to control the flow rate is to utilize the hydraulic resistance of a microfluidic channel. That is achieved by fine-tuning the channel's length, width, and depth. For example, a wider channel will provide a lower hydraulic resistance and allow for a higher flow rate. Flow rates can be adjusted from very slow flow (about 1.8 μL/min in fat tissue) to very fast (about 61.2 μL/min in lung tissue) (Miller & Shuler, 2016). When the angle the devices are placed on is significant (≈ 45° to ≈ 90°), the resulting flow can reach magnitudes that cause endothelial cells to align to the direction of flow (Fathi & Esch, 2022; Y. Yang et al., 2019). However, it should be noted that in systems that are operated using a rocker platform or a rotating platform the flow typically reaches its maximum at the beginning of the cycle and then decreases over time.

For the purpose of toxicity testing, especially for picking up secondary effects that result from the original exposure to a drug or other toxicant, and inter-organ interactions, the main advantage of pumpless MPS lies in the fact that those devices can recirculate very small amounts (almost near-physiological) of liquids (L. Chen et al., 2020). Since the average adult human body contains 5 L to 6 L of blood, an MPS that is scaled down by a factor of 50000 to 100000 should only contain about 50 μL to 120 μL of blood surrogate (cell culture medium) to replicate physiological values. Additional cell culture medium in each cell culture chamber is justified if its purpose is to mimic the interstitial fluid present in each organ. It is challenging to recirculate such small amounts of cell culture medium in an MPS, but some MPS designs can achieve it (L. Chen et al., 2020).

To benefit from testing a drug or nanoparticle with a pumpless MPS, a significant amount of thought has to go into its design and operation (see info box 1). For example, when operating a pumpless MPS with bidirectional flow, care must be taken to operate it with enough liquid such that no portion of the medium becomes trapped inside the fluidic circuit and becomes nutrient-depleted over time.

Alternatively, pumpless MPS can also be operated with unidirectional flow. Unidirectional flow systems must contain an active or passive valve mechanism that allows the cell culture medium to flow back to the top reservoir through a second fluidic path that does not lead through the organ chamber (Fig. 1 D-F) (L. Chen et al., 2020; Esch et al., 2016; Y. I. Wang & Shuler, 2018; Y. Yang et al., 2019). Unidirectional flow is important when the system contains barrier tissues such as the gastrointestinal tract epithelium or the endothelium since those tissues are sensitive to the direction and magnitude of shear. For example, the pattern of cell-cell junctions that regulate paracellular transport of drugs and nanoparticles can change when exposed to different levels of shear (Buchanan et al., 2014; Dabagh et al., 2017). To create significant amounts of shear inside microfluidic vessels lined with endothelial cells, the height difference between the system's reservoirs can be increased using custom-build rocker platforms (J. won Jeon et al., 2021; H. J. Song et al., 2017) or rotating platforms that place the MPS at angles of up to 90° (Fathi & Esch, 2022).

Both pumped and pumpless MPS can be used to better simulate the uptake, biodistribution, and elimination of drugs and nanoparticles *in vitro*. Multi-organ devices have also the potential to simulate inter-organ communication and to detect secondary drug toxicity stemming from toxic drug metabolites or adverse responses of tissues. Table 1 lists examples of both pumped and pumpless MPS that have been used to assess nanoparticles.

## 2. Pumped and PUMPLESS MPS FOR ASSESSING NANOPARTICLES

### 2.1 Uptake of nanoparticles

The uptake of nanoparticles into the body typically happens through exposure to the skin, the airways, or through oral ingestion. All three organs, the skin, the lung and the gastrointestinal tract (GI tract) have been modelled on microfluidic chips, sometimes in conjunction with other organ mimics (Fig. 2). Systems that provide access to both the apical and basolateral sides of the tissue are suitable for quantifying the passage of nanoparticles across those barrier tissues. Access is often achieved by culturing cells on porous, track-etched polymer membranes, similar to those used in transwells (Arlk et al., 2018; Zoio et al., 2021). Since such membranes are not as thin and as porous as *in vivo* basement membranes, alternatives made from other materials such as a thin layer of porous epoxy (Esch et al., 2012), and poly (lactic-co-glycolic acid) (PLGA) (X. Yang et al., 2018), as well as systems without membranes have been developed (M. Zhang et al., 2018). Using polydimethylsiloxane (PDMS) as membrane material has the added benefit that it is stretchable and well-suited to mimic mechanical forces that may affect barrier tissues (Huh et al., 2010).

Therapeutic nanoparticles can also be administered intravenously. Regardless of the route of administration, nanoparticles must cross the vascular endothelium if their intended targets

are beyond the vasculature. Because of their high relevance, models of the endothelium were among the first to be developed in an on-chip format.

**2.1.1 Uptake through the lungs—**Microfluidic systems have been used to re-create important components of the human lung alveolar-capillary interface that facilitates nanoparticle uptake through the airways. The lung epithelium contains cells that produce surfactants that keep the air-exposed apical side of the tissue covered with a thin layer of liquid thereby reducing surface tension and stabilizing it. The presence of surfactants influences the strength of the alveolar-capillary barrier (Frerking et al., 2001), and is likely responsible for its relatively high electrical resistance. The breathing motion of the lung also causes the lung epithelium to constantly stretch (5 % to 15 %), which has been shown to affect the permeability of the pulmonary endothelial cell barrier (Birukov et al., 2003; Birukova et al., 2006).

To recapitulate the characteristics of the lung alveolar-capillary interface in a pumped MPS, Huh et al. cultured lung epithelial cells in an MPS that contained a porous membrane and exposed the cells to air on their apical side and cell culture medium on their basal side (Huh et al., 2007). The air-exposed cells produce Clara cell 10 kDa protein (CC10), indicating that some cells in the system have differentiated into Clara cells. (Clara cell 10 kDa protein is involved in pulmonary surfactant biology as it binds surfactant lipids (Singh & Katyal, 1997)). Building on that lung model, but using stretchable PDMS membranes, Huh et al. were also able to additionally expose the lung epithelium to 10 % mechanical strain at a frequency of 0.2 Hz (Huh et al., 2010). Measurements after 4 h showed that the mechanical stress increased the translocation of 100 nm polystyrene nanoparticles from the apical to the basal side of the epithelial-endothelial layer while albumin permeability remained unchanged. Mechanical stress also contributed to the inflammatory response of the tissue to 12 nm silica nanoparticles (measured after 2 h of exposure) (Huh et al., 2010).

Cell-extracellular matrix (ECM) interactions in the lung have been modelled with a membraneless MPS where a layer of matrigel functioned as seeding surface for human pulmonary alveolar epithelial cells (HPAEpiCs) on one side and human umbilical vein endothelial cells (HUVECs) on the other (M. Zhang et al., 2018). While cell culture medium was pumped through the system at 10 μL/h, 25 nm $TiO_2$ and 40 nm ZnO nanoparticles were added at low and high concentrations to the pulmonary compartment (50 μg/mL, and 200 μg/mL respectively). The nanoparticles increased the barrier tissue's permeability to fluorescent dyes and ZnO particles also caused significant levels of apoptosis. However, it was noted that tissues that were constructed from only one of the two cell types (HUVECs or HPAEpiCs) were more susceptible to nanoparticle damage, highlighting the importance of cell-cell interactions in this lung tissue mimic.

**2.1.2 Uptake through the skin—**Native skin is highly complex, containing three distinct layers of tissues (epidermis, dermis, and hypodermis) that are each composed of several cell types. *In vitro* engineered 3D human skin constructs (HSCs) are used for testing cosmetics and pharmaceuticals. Static models of full thickness HSCs with several cell types, including keratinocytes, fibroblasts and melanocytes are already commercially available (Stojic et al., 2019). HSCs cultured under static conditions have been used for assessing skin

irritation caused by nanoparticles such as $TiO_2$ nanoparticles (Sanches et al., 2020) and $SiO_2$ nanoparticles (Wills et al., 2016), as well as the efficacy of anti-inflammatory drugs, such as dexamethasone loaded into nano-carriers (Graff et al., 2022).

Several on-chip, perfused skin models were developed recently (Ponmozhi et al., 2021; Risueño et al., 2021; J. Zhang et al., 2021). Perfused models offer the possibility to remove waste products from the tissue, to replenish nutrients, and to recruit cells and proteins that repair tissue damage from the stream of blood surrogate. Zhang et al. developed a high-throughput chip operated with external pumps to assess the cytotoxicity of small particles (2.5 μm or less in width) on epidermal cells (Y. Zhang et al., 2017). The study showed that such particles can upregulate the expression of interleukin-1β (IL-1β) and interleukin-6 (IL-6) and induce inflammation in epidermal cells. Despite lacking the dermis component, this system provides an example of how to use skin-on-chip MPS for screening of nanoparticles.

In 2015, Abaci et al. developed a pumpless microfluidic system which can maintain full-thickness HSCs at an air-liquid-interface culture for up to three weeks (Abaci et al., 2015). The model uses microchannels underlying the HSC compartment to achieve physiological blood residence times in human skin. Lee et al. further extended that design to generate HSCs *in situ* and demonstrate the critical role of fluidic flow for the long-term culture of HSCs (S. Lee et al., 2017). While the fluidic models and the static transwell models express similar amounts of proteins such as collagen IV and keratin 10, Song et al. suggested that static cultures in transwells dry quicker, leading to a higher degree of collagen matrix contraction (H. J. Song et al., 2018). In a recent study, Ronaldson-Bouchard et al. integrated HSCs onto a multi-organ platform containing bioengineered liver, heart, bone and vascular tissues, and studied the tissue-specific toxicity of doxorubicin on skin and other tissues (Ronaldson-Bouchard et al., 2022). The air-liquid-interface culture of HSCs was achieved using a floating device that could also be useful in future pumpless device designs.

Using a pumpless skin-on-a-chip model, Kim et al. demonstrated the testing of a cosmetic ingredient (*Curcuma longa* leaf extract) and its effects on gene expression levels of proteins involved in establishing the barrier function of skin (filaggrin, involucrin, laminin alpha-5, and keratin 10) (K. Kim et al., 2020). Building on previous work that optimized the extracellular matrix component of the system (H. J. Song et al., 2017), their skin model utilized rat tail collagen to support the 3D skin culture. A follow-up study with this fluidic skin model was able to recapitulate the side effects the kinase inhibitor sorafenib has on the skin (H. M. Jeon et al., 2020), showing that drug toxicity data can be replicated with such systems.

Fluidic flow underneath the *in vitro* skin model also enables the culture of endothelial cells that can then be exposed to fluidic shear. Wufuer et al. developed a pumpless model where fibroblasts and HUVECs were cultured on opposite sides of a porous membrane where medium flow was possible on both sides (Wufuer et al., 2016). This culture was combined with another membrane culture that held keratinocytes and fibroblasts on opposite sides. The model could reproduce the protective effects of dexamethasone on the tight junctions of HUVEC layers when dexamethasone was added to the keratinocyte layer and the HUVEC

were challenged with inflammation-inducing tumour necrosis factor-α (TNF-α). However, this model (as all current pumpless on-chip skin models) was cultured under bidirectional fluidic flow that can create higher levels of inflammation in HUVEC (Y. Yang et al., 2019). Using unidirectional flow designs (Fig. 1D-F) may be suitable to decrease the baseline inflammation exhibited in the system. So far none of the pumpless skin MPS has been exposed to nanoparticles yet.

**2.1.3 Oral uptake and first pass through the liver—**The oral uptake of nanoparticles into the systemic circulation requires the particle's travel through the gastrointestinal tract, crossing the intestinal mucous and epithelial cell layers, and passing through the liver without being captured by Kupffer cells. To estimate the fraction of nanoparticles that make it into the bloodstream, Esch et al. (Esch et al., 2014) have used a pumped MPS with GI tract epithelium and liver tissue models that simulated the oral uptake and first pass through the liver albeit without Kupffer cells. The GI tract module contained a mixture of intestinal epithelial cells (Caco-2) that developed 2D cell layers with tight junctions and cells that produce mucous (HT29-MTX) (Mahler et al., 2009). A similar system was tested earlier with acetaminophen, showing that the concentrations of acetaminophen metabolites increase over time in the systemic circulation of the MPS. A test with 50 nm carboxylated polystyrene nanoparticles (NP) (240 x $10^{11}$ NP/ mL and 480 x $10^{11}$ NP/ mL) suggested that the GI tract mucous layer and epithelium presents an effective barrier to the majority of the particles (90.5 % ± 2.9 %), and that the particles that do cross the barrier emerge with a changed zeta potential (Esch et al., 2014). In that study, the flow on both sides of the membrane on which epithelial cells grew was driven with external peristaltic pumps that were carefully balanced to avoid a large pressure drop across the GI tract tissue. Shinha at el. achieved a balanced fluidic flow with system-integrated micropumps as well (Shinha et al., 2021).

A pumpless system that incorporates the GI tract epithelium as well as liver tissue was published in 2016 by Esch et al. (Esch et al., 2016). That system was capable of sustained GI tract and liver cell co-culture in a mixture of cell culture medium for fourteen days. Another pumpless version was published in 2021 by Jeon et al. (J. won Jeon et al., 2021), who used it to evaluate the absorption of fatty acids and reproduced the anti-steatotic effects of turofexorate isopropyl (XL-335) and metformin. These pumpless MPS have not yet been used to simulate the oral uptake of nanoparticles.

**2.1.4 Uptake through the Endothelium—**Nanoparticles that are administered intravenously, or that reach the systemic circulation after entering uptake through the GI tract, the lung, or the skin can cross the endothelium. The endothelium is a monolayer of endothelial cells that line the blood-facing side of blood vessels. Endothelial cells connect with each other via junction proteins, creating an effective physical barrier. Since fluidic flow influences the morphology of endothelial cells and with that the cell layer's permeability (Buchanan et al., 2014), fluidic models may be better suited to quantify nanoparticle travel across the endothelial barrier than static models. Microfluidics can be used to recreate both the mechanical and chemical factors that influence the vascular microenvironment (ABACI et al., 2013). Early microfluidic models of the endothelium

utilize polydimethylsiloxane (PDMS) and large glass cover slips to construct microchannels that are lined with HUVEC (Esch, Post, et al., 2011). The endothelial linings can be exposed to varying magnitudes of shear, mimicking the varying conditions the cells encounter *in vivo*. Instead of PDMS, dense collagen matrixes can also be used as channel material (Alimperti et al., 2017; Cross et al., 2010; Tronolone et al., 2021), making it possible to observe substance transport across the endothelial barrier into the extracellular matrix (ECM).

A drawback of those early models was that they were operated with external pumps to drive unidirectional fluidic flow, but without liquid recirculation. At high flow rates this one-time pass technique creates significant waste of cell culture medium. In 2017, Van Duinen et al. published a commercially available cell culture plate that contained 96 microfluidic perfusable vessels that were lined with endothelial cells (van Duinen et al., 2017). Recirculating medium flow within the vessels is driven by gravity when the plate is placed on a rocker platform. Medium flow through the vessels changes direction every 8 min with the highest magnitude of shear reaching 0.5 Pa (5 dyn/cm$^2$) right after the rocker position changes.

In addition to the templated models described above (where the vessel structure is microfabricated and then lined with cells), there are also self-organized networks of capillaries where vessel networks form within 4 days to 7 days of mixing stromal cells and endothelial cells within a polymerized hydrogel (Traore & George, 2017). Such vessel networks can be perfused with pressure-driven flow (S. Kim et al., 2013; Moya et al., 2013; J. W. Song et al., 2012) or with gravity-driven flow (Chan et al., 2012; Yeon et al., 2012). Self-organized vessel networks are particularly useful when studying vessel formation in response to varying biochemical and biophysical growth conditions (Ehsan & George, 2015).

To create pumpless vessel perfusion systems that can generate unidirectional medium flow, Wang et. al and Yang et al. have developed systems that redirect the fluidic flow to the top medium reservoir through a secondary channel (Y. I. Wang & Shuler, 2018; Y. Yang et al., 2019). Yang et al. used their system to compare HUVECs grown under bidirectional and unidirectional fluidic flow, showing that bidirectional flow causes the cells to release higher concentrations of inflammatory cytokines (Y. Yang et al., 2019). Inflammation can change the structure of tight junctions and adherens junctions and increase endothelial leakiness (Claesson-Welsh et al., 2021). A model of the lymph node endothelium reacted similarly to bidirectional medium flow (Fathi & Esch, 2022).

The magnitude of shear created within MPS can influence nanoparticle uptake into the endothelium as shown by Samuel et al. who tested negatively charged 2.7 nm and 4.7 nm CdTe quantum dots and 50 nm $SiO_2$ nanoparticles under several magnitudes of shear (0 Pa, 0.05 Pa, 0.1 Pa, and 0.5 Pa) (Samuel et al., 2012). Fede et al. also observed that HUVECs exposed to 13 nm gold nanoparticles remained more viable when the exposure occurred under fluidic flow (5 μL/min for 24 h) rather than in transwells, even though the overall number of nanoparticles administered in the fluidic system was higher (Fede et al., 2015, 2017).

Microfluidic vessel networks have also been used to recreate organ-specific models of the vasculature with their distinct characteristics (Herron et al., 2019). For example a model of the vasculature was integrated with heart and liver tissues in the HeLiVa device (Vunjak-Novakovic et al., 2013). Among tissue-specific blood vessel models, the blood brain barrier (BBB) is particularly difficult to achieve because of its high transepithelial resistance (TEER) and low rates of transcytosis. The BBB prevents the transport of large drugs and antibodies into the brain. A number of fluidic models of the BBB already exist (Berry et al., 2018) with at least one utilizing a pumpless platform (Y. I. Wang, Erbil Abaci, et al., 2017). Pumped BBB chips developed by Papademetriou et al. show that angiopep-2 coated liposomes (80 nm to 95 nm in diameter) bind to brain endothelial cells under static conditions and at low flow (0.1 Pa) but not at higher flow rates (0.6 Pa) (Papademetriou et al., 2018). Considering that shear in the brain is estimated to be between 0.5 Pa to 2.3 Pa (Cucullo et al., 2013; Jamieson et al., 2017), their study demonstrates the importance of testing nanoparticle uptake under fluidic flow. Similarly, Park et al. were able to recapitulate the shuttling activities of angiopep-2 using their model of the BBB and angiopep-2 coated quantum dots (20 nm in diameter) (Park et al., 2019). The BBB model was constructed from induced pluripotent stem cell-derived human brain microvascular endothelial cells that were differentiated using a developmentally inspired protocol that included temporary hypoxic conditions. The model also contained primary human brain astrocytes and pericytes and mimicked the barrier function of the *in vivo* BBB well, including higher impedance values (about 24000 Ω after two days of culture) when compared with the same differentiation protocol conducted in transwells.

## 2.2 Biodistribution

Multi-organ MPS that mimic the human body can potentially be used to study the biodistribution of nanoparticles in the human body. However, the design of multi-organ MPS strongly influences how a drug or substance is distributed within it, and to obtain useful predictions, that design must be carefully considered. Since the inception of multi-organ MPS, design criteria have been discussed with some researchers proposing to use physiologically based pharmacokinetic models and physiologically based tissue volume ratios as guiding principles (Esch, King, et al., 2011; Malik et al., 2021; Sung, Esch, et al., 2010; Sung et al., 2020). When following those guidelines, organ-specific flow rates create fluid residence times that may mimic the *in vivo* exposure of a tissue to nanoparticles.

Several pumpless multi-organ MPS have been developed(L. Chen et al., 2020; LaValley et al., 2021; H. Lee et al., 2017; H. Li et al., 2022; Miller & Shuler, 2016; Oleaga et al., 2016). Miller et al. built a 14-organ system, demonstrating it with five living tissues (Miller & Shuler, 2016). However, most multi-organ MPS contain a limited number of organ chambers. When organs are left out, the implicit assumption is that drugs or nanoparticles do not interact with those organs, meaning they are not absorbed, metabolized, or excreted in significant amounts by those organs.

To achieve physiological values, the blood surrogate volume in a multi-organ MPS can be scaled using the same scaling factor as was used for all other organs in the system. However, such a design requirement can be difficult to implement since MPS tissues tend to be quite

small (typically 1/50000$^{th}$ to 1/100000$^{th}$ of the human organ). The body cube developed by Chen et al. demonstrated the co-culture of four tissues with physiologically scaled amounts of blood surrogate (i.e. 80 μL of recirculating cell culture medium in a system that was scaled down using a scaling factor of 73000) (L. Chen et al., 2020). That was achieved by arranging the cell culture chambers in a cube format so that fluidic connections between organ chambers were short and the amount of liquid needed to operate the device could be decreased to 80 μL (1/73000 of the physiological volume of blood).

On the other hand, currently most pumpless multi-organ MPS are operated using bidirectional fluidic flow, making it necessary to ensure that there is enough medium inside the device so that none of it becomes trapped in the channel network of the device. Trapping even small amounts of medium inside the system will result in nutrient depletion in the middle of the device and potentially cause unexpected adverse effects in the tissues residing there. Small-scale MPS that recirculate small amounts of liquid are also prone to liquid evaporation, making it necessary to replace evaporated amounts regularly. Evaporation is deleterious to cell culture in microfluidic systems because it significantly increases osmolality, affecting cell physiological characteristics including cell metabolism (Yun et al., 2007).

Unidirectional flow systems are needed when tissues that are exposed to significant shear inside the body, such as the vasculature, are included in the multi-organ MPS. A number of passive device designs that direct the fluidic flow in a single direction even when the device is operated on a rocker platform have been developed (Esch & Shuler, 2015; Y. I. Wang & Shuler, 2018; Y. Yang et al., 2019), (Fig. 1), including one multi-organ system (LaValley et al., 2021).

However, despite their potential capability none of the multi-organ MPS has been used yet for nanoparticle distributions studies.

## 2.3 Elimination

**2.3.1 Liver—**Because of its central role in drug metabolism and drug toxicity studies, liver tissue was one of the first to be constructed as an MPS (Sin et al., 2008; Viravaidya et al., 2008) and one of the first to be created in a pumpless MPS (Sung, Kam, et al., 2010). Pumped liver MPS have been used to recapitulate liver architecture, liver zonation, and liver disease models (P. Y. Chen et al., 2021; Decsi et al., 2019; Y. B. A. Kang et al., 2015; Moradi et al., 2020; Polidoro et al., 2021; Prot et al., 2012). For nanoparticle biodistribution and toxicity testing, it is useful to incorporate Kupffer cells into the MPS liver tissue. Kupffer cells are resident macrophages in the liver that remove particulates and foreign matter from the portal vein through phagocytosis (Dixon et al., 2013). They are responsible for sequestering significant amounts of nanoparticles (15 nm to 200 nm in size), changing the number of particles in the liver and in circulation (MacParland et al., 2017; Poon et al., 2019) and with that their toxicity profiles (Zhu et al., 2017).

To build a liver functional unit with *in vivo*-like 3D architecture, multiple cell types and extracellular matrix have been used (Bhushan et al., 2013; Esch et al., 2015). Fluidic flow at physiological flow rates across liver tissue has been shown to increase liver metabolism

(Esch et al., 2015), which is likely due to an increase in the rate of gas exchange under flow (Rennert et al., 2015). Oxygen gradients across liver tissue can be created using a number of different MPS designs (Y. B. Kang et al., 2020; Y. B. A. Kang et al., 2018).

Some liver MPS have been exposed to nanoparticles for toxicity measurements (Jiang et al., 2021; L. Li et al., 2019). Pumpless liver MPS have not yet been used to test nanoparticles, but the systems are well-suited to probe particle elimination by Kupffer cells under physiological flow rates.

**2.3.2 Spleen—**Besides being trapped in the skin and liver, significant amounts of nanoparticles can also accumulate in the spleen either by being taken up by splenic macrophages in the white pulp section (particles that are 15 nm to 200 nm in size), or by being retained in the red pulp section and internalized by macrophages there (particles that are larger than 200 nm) (Almeida et al., 2011; Moghimi et al., 2001). The red-pulp zone and the white pulp zone of the spleen are separated by the perifollicular zone. The spleen has interendothelial slits (IES) that hold back blood-borne pathogens, aging red blood cells as well as larger nanoparticles (100 nm and larger). *In vivo* IES can be between 250 μm to 1200 μm wide openings with an average length of 1.89 μm (Deplaine et al., 2011), a slit size that can easily be microfabricated with contact photolithography methods. Microfluidic chips that mimic those slits have been made to filter out larger cells such as circulating tumor cells and to investigate mechanical deformation of human cells (Patil et al., 2015). However, there are currently very few microfluidic chips that mimic the IES of the spleen as well as the physiological flow division. Rigat-Brugarolas et al. fabricated a pumped microfluidic device that is operated without human cells, but that accurately replicates the physiological flow division into fast flow and slow microcirculations (Rigat-Brugarolas et al., 2014). Picot et al. also designed a fluidic chip with slits that they tested with red blood cells, finding that infected cells were retained by the slits (Picot et al., 2015). Using a similar idea, an artificial microfluidic spleen device was developed and used to clean the blood of actual patients (J. H. Kang et al., 2014).

**2.3.3 Kidney—**Kidney MPS can provide a platform for testing and optimizing nanoparticle drug delivery systems. Circulating nanoparticles are cleared from the body by the organs of the reticuloendothelial system (RES) or the kidneys (Du et al., 2018). The kidneys are responsible for filtration, osmoregulation and reuptake, and receive about 25 % of cardiac output, meaning that they play a large role in absorption, distribution, metabolism, elimination, and toxicity (ADMET) of a substance (Brown et al., 1997). Major components of the nephron, which are the functional units of the kidney, include the glomerulus, proximal tubule, distal tubule, and collecting duct. The glomerulus is a network of capillaries surrounded by Bowman’s capsule. The glomerular filtration membrane is composed of glomerular endothelial cells, a basement membrane or basal lamina, and podocytes. Together, this structure is responsible for the size- and charge-dependent filtration of blood (Marieb & Hoehn, 2019). Glomerular filtrate next reaches the proximal convoluted tubule, which is primarily responsible for the reuptake of salts, sugar, and water from the filtrate. This reabsorption is achieved through both active and passive transport. Within the distal tubule, charged particles can be transported into and out of the filtrate,

and finally concentrated filtrate reaches the collecting ducts for transport to the bladder for removal from the body (Marieb & Hoehn, 2019). During the reabsorption process urine becomes highly concentrated, allowing for the toxicity of compounds to emerge (Bonventre et al., 2010). Due to their function the majority of drug toxicity cases (90 %) occur within the proximal tubule and glomerular regions of the kidney (Bonventre et al., 2010), which has also made glomerulus and proximal tubules the focus of MPS development. Nanoparticles are quickly filtered from the blood, and important considerations in nanomedicine design is renal clearance (Du et al., 2018).

The glomerular filtration barrier (GFB) filters approximately 180 L of blood daily, and filtration is dependent on both size and charge of a compound (Comper & Glasgow, 1995; Gallardo & Vio, 2022; Tencer et al., 1998). Nanoparticle interaction with the GFB is dependent on particle density, size, material, structure, and charge. Low density nanoparticles such as silica particles circulate faster in the blood stream, are more easily distributed in the body, have lower renal accumulation, and have faster renal clearance when compared with more dense particles such as gold nanoparticles (Huang et al., 2021; Tang et al., 2016). Nanoparticles with a size below 10 nm (30 kDa to 50 kDa) are able to pass through the glomerulus and enter the proximal tubule (Huang et al., 2021). Larger particles (10 nm to 20 nm) made from soft organic polymer-based materials can squeeze through glomerular pores. Positively charged nanoparticles can pass through the GFB more easily than negatively charged nanoparticles due to electrostatic repulsion, and disk or rod-like nanomaterials have a longer circulation half-life when compared with spherical nanoparticles (Huang et al., 2021). A number of glomerulus MPS have been developed with rodent (L. Wang et al., 2017; Zhou et al., 2016) or human cells (Musah et al., 2017; Petrosyan et al., 2019). Musah et al. were able to demonstrate that human-induced pluripotent stem cell-derived podocyte-like cells cultured with human glomerular endothelial cells secreted glomerular basement membrane collagen and differentially filtered albumin and inulin. The two channel MPS used a vacuum device which pulled the fluid through the device (Musah et al., 2017).

In the proximal and distal tubules, water, ions, and small molecules can be reabsorbed from the filtrate into the circulation, and unwanted ions and molecules can be removed from the bloodstream and secreted into the filtrate via ATPase pumps or passive diffusion (Marieb & Hoehn, 2019). Tubular secretion can also be used to remove nanoparticles greater 100 nm from the bloodstream, where the nanoparticles are secreted from the bloodstream into the filtrate via exocytosis (Deng et al., 2019; Huang et al., 2021). Proximal and distal tubule and collecting duct MPS have been developed with both human and animal cells (Fig. 2), although flow is driven through these systems with a pump (Mahler & Zhang, 2021). Pump-driven MPS of both the proximal tubule and glomerulus have also been reported (Sakolish et al., 2019; Sakolish & Mahler, 2017; S. Y. Zhang & Mahler, 2021, 2022). Kidney tissue slices (Bartucci et al., 2020) and 3D kidney organoids (Astashkina et al., 2014) have been used for nanoparticle toxicity testing, but kidney MPS have not, to date, been used.

Few studies have focused on the development of a pumpless kidney MPS. A 3D printed paper-based system created by Li et al. contains cells seeded into set chambers for individual organ types (H. Li et al., 2022). This system also incorporates a hydrogel (GelMA) as a

matrix for cell seeding. With viability studies producing strong results after seven days, the technology has the potential to be scaled up for large-scale toxicity testing. This MPS uses gravity along with capillary action of its small vascular channels to facilitate system flow. With the initial drug and medium being placed in a siphon reservoir, medium can move through the entire MPS. The ease of printing and ability to make fast changes allows for flow to be highly controlled and editable, and this system could be used to model components of the kidney.

### 2.4 Toxicity measurements

In 2008, Lewinski et al. summarized *in vitro* cytotoxicity data for nanoparticles that were available then, finding that cytotoxic effects emerge in a dose- and time-dependent manner for all the nanoparticles they reviewed. MPS can contribute to uncovering cytotoxicity and also help determine functional changes of tissues in response to nanoparticle exposure. For example, Ahn et al. demonstrated that exposure to high doses of $TiO_2$ nanoparticles (29 nm ± 11 nm in diameter) and Ag nanoparticles (22 nm ± 3 nm in diameter) disrupts the contractile function of cardiac tissue through structural damage to tissue architecture (S. Ahn et al., 2018). The study provides evidence of MPS as a platform for conducting physiologically relevant nanotoxicology studies of 3D cardiac tissues. A study by Lu et al., also suggests that CuO nanoparticles can disrupt the endothelial barrier which affects the particle's translocation to cardiac tissue (Lu et al., 2021). The particles induce electrical and contractile dysfunction through the generation of reactive oxygen species (ROS) and subsequently cause disruption of cardiac troponin T and secretion of biomarkers associated with cardiac injury (B-type natriuretic peptide, N-terminated pro-hormone BNP, and troponin I). $SiO_2$ nanoparticles elevate the secretion of pro-inflammatory cytokines and alter the intercellular $Ca^{2+}$ handling (Lu et al., 2021).

In a study conducted by Li et al., exposure to atmospheric nanoparticles (ANPs) caused endothelial dysfunction, including increased vessel permeability by disrupting endothelial cell tight junctions. ANPs also caused imbalance in the intravascular expression of vasoconstrictors and vasodilators, increased levels of inflammation, and increased $Ca^{2+}$ influx. The results suggest that this 3D human microvessel model is suitable for the evaluation of vascular toxicity after human vessel exposure to nanoparticles (Y. Li et al., 2019).

Liver MPS have also been used to assess nanoparticle toxicity (Esch et al., 2014) and the effects of nanoparticles on albumin and urea production (L. Li et al., 2019). Li et al. exposed liver tissue grown in an MPS to 10 nm superparamagnetic $Fe_3O_4$ nanoparticles, finding that fluidic flow increases the tissue's sensitivity to the particles, which is expressed in a decreased production of albumin. Jiang et al. have also used a liver MPS with liver spheroids to probe the toxicity of CuS nanoparticles (Jiang et al., 2021). The particles caused a decrease in spheroid viability, albumin and urea production and glycogen deposition. CuS particles also altered the mitochondrial membrane potential and caused an increase in the production of reactive oxygen species.

Multi-organ MPS also have the potential to detect secondary effects that arise after nanoparticle exposure due to the recirculation of soluble components among all tissues

cultured within the system. Here, the amount of blood surrogate present in the MPS can influence the severity of such effects. Systems that contain physiologically scaled amounts of blood surrogate (as discussed in section 2.2) are likely most suitable to pick up such secondary effects.

## 3. Outlook

The most important difference between traditional *in vitro* tissue models and fluidic MPS is the presence of fluidic flow. The flow of medium has been shown to affect *in vitro* tissues in several ways. For example, while human skin constructs express similar amounts of proteins such as collagen IV and keratin 10 in fluidic models and in static transwell models, Song et al. found that static cultures in transwells simply dry quicker, leading to a higher degree of collagen matrix contraction and shorter viability of the tissue (H. J. Song et al., 2018). In a liver MPS, fluidic flow was shown to increase the metabolism in heptocytes (Esch et al., 2015) likely as a consequence of increased rates of gas exchange that become possible under flow (Rennert et al., 2015).

In the context of testing nanoparticles, the most significant effects of fluidic flow are that the barrier function of models of barrier tissues typically increases under fluidic flow. For example, a model of the BBB that was constructed from stem cells was capable of reaching much higher impedance values (about 24000 Ω after two days of culture) compared with the same model grown in transwells (Park et al., 2019). The difference flow makes in nanoparticle uptake across models of the endothelium constructed from HUVEC has been quantified by several groups. Samuel et al. who used negatively charged 2.7 nm and 4.7 nm CdTe quantum dots and 50 nm $SiO_2$ nanoparticles and several different magnitudes of shear (0 Pa, 0.05 Pa, 0.1 Pa, and 0.5 Pa) showed that nanoparticle uptake was highest at low flow conditions and decreased at higher flow rates (Samuel et al., 2012). Similarly, Fede et al. found that 13 nm gold nanoparticle accumulation in endothelial cell layers is very low (0.17 %) under flow compared to accumulation in wells (29.2 %) (Fede et al., 2015, 2017).

Fede et al. point out that the number of total administered nanoparticles in a flow system without recirculation is much higher than that in wells without flow. As an example, in their system a concentration of $1 \times 10^{12}$ nanoparticles/mL flown at a flow rate of 5 μL/min for 24 h, the number of administered nanoparticles is $1.5 \times 10^{8}$ nanoparticles/cell in fluidic device compared with $1 \times 10^{7}$ nanoparticles per cell in the well (Fede et al., 2017). Here, pumpless fluidic devices that can recirculate small amounts of medium could offer a solution to creating a more equal exposure to nanoparticles.

Fluid recirculation in MPS can also reduce medium waste (compared to one-pass systems) and allow the MPS to be used for testing small amounts of expensive compounds. In the case of nanoparticles, recirculation would allow for particles to remain in the system for a defined exposure time.

Another feature of MPS that has been shown to influence nanoparticle uptake is mechanical stretching of tissues such as the alveolar-capillary interface. For example, the uptake of 100 nm polystyrene particles by lung epithelial cells was significantly increased when the tissue

was stretched 10 % at a frequency of 0.2 Hz (Huh et al., 2010). Stretching of tissues have previously been accomplished with more traditional tissue models, but MPS can combine stretching and fluidic flow to mimic the *in vivo* situation more fully.

Multi-organ MPS where multiple tissues are incorporated into the same system to mimic the human body may also provide an opportunity to test nanoparticles in a complex environment. Nanoparticles may acquire a lipid/protein coating (for example by crossing the GI tract epithelium) that could influence their interaction with other tissues. However, current obstacles to using multi-organ MPS for nanoparticle testing are similar to those for testing other drug candidates (Andersen et al., 2014; Hargrove-Grimes et al., 2022; Livingston et al., 2016; Starokozhko & Groothuis, 2017). Most importantly, to accurately mimic the human body, MPS – especially multi-organ MPS with recirculating medium flow – remain very complex. To construct tissues that mimic the *in vivo* tissues in terms of architecture and function, multi-cell type 3D models made from primary cell sources or stem cell sources are best used. Those cell types require specialized medium formulations and to culture multiple tissues within one MPS, those medium formulations must be optimized to suit all tissues, a task that becomes more difficult the more tissues are included in the MPS.

Depending on the objective of the measurements, the MPS must be designed to deliver outputs that are suitable to inform further development options, such as determining suitable nanoparticle candidates and perhaps concentration ranges. Here, challenges remain with increasing device complexities of multi-organ MPS. A device that includes one or several barrier tissues becomes a complex system that requires several microfluidic circuits representing, for example, the apical side of the GI tract, the systemic circulation of the body, and the basolateral side of the kidney. A multi-circuit-device must retain balanced fluidic flow so that the pressure exerted on barrier tissues remains within physiological limits. Here, pumpless system components may be able to better provide the needed complexity.

While MPS offer many possibilities, there are also some interactions of nanoparticles with the human body that are not easily modelled *in vitro* and where *in vivo* testing is still needed. For example, nanoparticle interactions with components of the immune system can potentially be studied with MPS to examine the fate of nanoparticles in the presence of immune responses, but studies to that effect have not yet been conducted (Maharjan et al., 2020). Nanoparticles have also been shown to cause some physiological changes such as an increase of intestinal villi sizes upon exposure (Mahler et al., 2012). Such physiological changes may not be observed within MPS and in those cases experiments with MPS can only guide more in-depth *in vivo* test.

One goal for MPS developers is to reduce the use of animals in the drug development process by either eliminating drug candidates early in the development process (before animal experiments), or by decreasing the parameter space that needs to be evaluated with animals. Ideally, in the future, MPS would mimic the human body in a way that can achieve those goals. In addition, to evaluate MPS responses, device validation should be possible. To that effect there are several groups who currently are working to provide such validation methods for MPS. However, the development of MPS is still an active field of research and

the best strategies to design and use the devices are still under debate. The adoption by industry also likely depends on the cost of MPS, which can be significant. Here, pumpless devices may offer the benefit of being less expensive, easier to manufacture, and easier to operate while still delivering some key requirements.

## 4. Conclusion

MPS are well-suited for drug and nanoparticle testing. Devices that contain barrier tissues such as a mucosal layer, an epithelium, or an endothelium can be used to estimate the uptake and bioavailability of nanoparticles in the systemic circulation. MPS offer the opportunity to test those processes under fluidic flow and when tissues are exposed to mechanical forces such as mechanical stretching. Devices that contain elements of the liver, spleen, or kidney offer the possibility to estimate nanoparticle elimination from the body, though more work needs to be done in this area to further demonstrate this capability. Similarly, multi-organ MPS that contain tissues that interact with nanoparticles may be suitable to estimate their biodistribution within the body, though this has not been achieved yet. Pumpless MPS could contribute to nanoparticle testing with MPS by simplifying the design and operation of complex multi-organ systems that require multiple fluidic circuits. They can also provide the capability to study nanoparticles in systems with near-physiological fluid volumes and under recirculating fluid flow rather than one-pass flow systems. Both pumped and pumpless MPS can used to study nanoparticles in a systematic way to determine best materials, sizes, shapes, and surface coatings. In this way, MPS may contribute to reducing necessary animal experiments, though certain aspects of nanoparticle testing with animals might remain necessary.

## Acknowledgments

We thank Ruth Ann Cho for creating the illustration of the human body in Figure 2.

### Funding Information

G. J. Mahler and Z. Krassin acknowledge financial support from the National Institutes of Health (NIEHS) (R01 ES028788) and the Graduate Fellowship for STEM Diversity. Eun-Jin Lee acknowledges support under the Professional Research Experience Program Agreement between the University of Maryland and the National Institute of Standards and Technology, agreement #70NANB18H165.

## References

ABACI HE, DRAZER G, & GERECHT S (2013). RECAPITULATING THE VASCULAR MICROENVIRONMENT IN MICROFLUIDIC PLATFORMS. 10.1142/S1793984413400011, 03(01), 1340001. 10.1142/S1793984413400011

Abaci HE, Gledhill K, Guo Z, Christiano AM, & Shuler ML (2015). Pumpless microfluidic platform for drug testing on human skin equivalents. Lab on a Chip, 15(3), 882–888. 10.1039/c4lc00999a [PubMed: 25490891]

Ahn S, Ardona HAM, Lind JU, Eweje F, Kim SL, Gonzalez GM, Liu Q, Zimmerman JF, Pyrgiotakis G, Zhang Z, Beltran-Huarac J, Carpinone P, Moudgil BM, Demokritou P, & Parker KK (2018). Mussel-inspired 3D fiber scaffolds for heart-on-a-chip toxicity studies of engineered nanomaterials. Anal Bioanal Chem, 410(24), 6141–6154. 10.1007/s00216-018-1106-7 [PubMed: 29744562]

Ahn SI, Sei YJ, Park HJ, Kim J, Ryu Y, Choi JJ, Sung HJ, MacDonald TJ, Levey AI, & Kim YT (2020). Microengineered human blood–brain barrier platform for understanding nanoparticle transport mechanisms. Nature Communications, 11(1). 10.1038/s41467-019-13896-7

Alimperti S, Mirabella T, Bajaj V, Polacheck W, Pirone DM, Duffield J, Eyckmans J, Assoian RK, & Chen CS (2017). Three-dimensional biomimetic vascular model reveals a RhoA, Rac1, and N-cadherin balance in mural cell–endothelial cell-regulated barrier function. Proceedings of the National Academy of Sciences of the United States of America, 114(33), 8758–8763. 10.1073/pnas.1618333114 [PubMed: 28765370]

Almeida JPM, Chen AL, Foster A, & Drezek R (2011). In vivo biodistribution of nanoparticles. In *Nanomedicine* (Vol. 6, Issue 5). 10.2217/nnm.11.79

Andersen ME, Betts K, Dragan Y, Fitzpatrick S, Goodman JL, Hartung T, Himmelfarb J, Ingber DE, Jacobs A, Kavlock R, Kolaja K, Stevens JL, Tagle D, Lansing Taylor D, & Throckmorton D (2014). Developing microphysiological systems for use as regulatory tools--challenges and opportunities. ALTEX, 31(3), 364–367. 10.14573/altex.1405151 [PubMed: 25061900]

Arlk YB, van der Helm MW, Odijk M, Segerink LI, Passier R, van den Berg A, & van der Meer AD (2018). Barriers-on-chips: Measurement of barrier function of tissues in organs-on-chips. Biomicrofluidics, 12(4). 10.1063/1.5023041

Astashkina AI, Jones CF, Thiagarajan G, Kurtzeborn K, Ghandehari H, Brooks BD, & Grainger DW (2014). Nanoparticle toxicity assessment using an invitro 3-D kidney organoid culture model. Biomaterials, 35(24). 10.1016/j.biomaterials.2014.04.060

Bartucci R, Paramanandana A, Boersma YL, Olinga P, & Salvati A (2020). Comparative study of nanoparticle uptake and impact in murine lung, liver and kidney tissue slices. Nanotoxicology, 14(6). 10.1080/17435390.2020.1771785

Berry D, Loy A, Coburn B, Guttman DS, Luca F, Kupfer SS, Knights D, Khoruts A, Blekhman R, Matsen FA 4th, McBain AJ, O'Neill CA, Amezquita A, Price LJ, Faust K, Tett A, Segata N, Swann JR, Smith AM, … Kiers ET (2018). Organ-On-A-Chip in vitro Models of the Brain and the Blood-Brain Barrier and Their Value to Study the Microbiota-Gut-Brain Axis in Neurodegeneration. Current Opinion in Biotechnology, 13(5), 247–257. 10.1038/s41477-018-0139-4

Bhushan A, Senutovitch N, Bale SS, McCarty WJ, Hegde M, Jindal R, Golberg I, Berk Usta O, Yarmush ML, Vernetti L, Gough A, Bakan A, Shun TY, Biasio R, & Lansing Taylor D (2013). Towards a three-dimensional microfluidic liver platform for predicting drug efficacy and toxicity in humans. In *Stem Cell Research and Therapy* (Vol. 4, Issue SUPPL.1). 10.1186/scrt377

Birukov KG, Jacobson JR, Flores AA, Ye SQ, Birukova AA, Verin AD, & Garcia JGN (2003). Magnitude-dependent regulation of pulmonary endothelial cell barrier function by cyclic stretch. American Journal of Physiology - Lung Cellular and Molecular Physiology, 285(4 29–4). 10.1152/ajplung.00336.2002

Birukova AA, Chatchavalvanich S, Rios A, Kawkitinarong K, Garcia JGN, & Birukov KG (2006). Differential regulation of pulmonary endothelial monolayer integrity by varying degrees of cyclic stretch. American Journal of Pathology, 168(5), 1749–1761. 10.2353/ajpath.2006.050431 [PubMed: 16651639]

Bonventre J. v., Vaidya VS, Schmouder R, Feig P, & Dieterle F (2010). Next-generation biomarkers for detecting kidney toxicity. In Nature Biotechnology (Vol. 28, Issue 5). 10.1038/nbt0510-436

Brown RP, Delp MD, Lindstedt SL, Rhomberg LR, & Beliles RP (1997). Physiological parameter values for physiologically based pharmacokinetic models. Toxicology and Industrial Health, 13(4). 10.1177/074823379701300401

Buchanan CF, Verbridge SS, Vlachos PP, & Rylander MN (2014). Flow shear stress regulates endothelial barrier function and expression of angiogenic factors in a 3D microfluidic tumor vascular model. Cell Adhesion and Migration, 8(5), 517–524. 10.4161/19336918.2014.970001 [PubMed: 25482628]

Chan JM, Zervantonakis IK, Rimchala T, Polacheck WJ, Whisler J, & Kamm RD (2012). Engineering of In Vitro 3D Capillary Beds by Self-Directed Angiogenic Sprouting. PLoS ONE, 7(12). 10.1371/journal.pone.0050582

Chen HJ, Miller P, & Shuler ML (2018). A pumpless body-on-a-chip model using a primary culture of human intestinal cells and a 3D culture of liver cells. Lab on a Chip, 18(14), 2036–2046. 10.1039/C8LC00111A [PubMed: 29881844]

Chen L, Yang Y, Ueno H, & Esch MB (2020). Body-in-a-Cube: a microphysiological system for multi-tissue co-culture with near-physiological amounts of blood surrogate. Microphysiological Systems, 4. 10.21037/mps-19-8

Chen PY, Hsieh MJ, Liao YH, Lin YC, & Hou Y te. (2021). Liver-on-a-chip platform to study anticancer effect of statin and its metabolites. Biochemical Engineering Journal, 165. 10.1016/j.bej.2020.107831

Chen YY, Syed AM, MacMillan P, Rocheleau J. v, & Chan WCW (2020). Flow Rate Affects Nanoparticle Uptake into Endothelial Cells. Adv Mater, 32(24), e1906274. 10.1002/adma.201906274 [PubMed: 32383233]

Cho KW, Lee WH, Kim BS, & Kim DH (2020). Sensors in heart-on-a-chip: A review on recent progress. Talanta, 219. 10.1016/j.talanta.2020.121269

Cho S, Islas-Robles A, Nicolini AM, Monks TJ, & Yoon JY (2016). In situ, dual-mode monitoring of organ-on-a-chip with smartphone-based fluorescence microscope. Biosens Bioelectron, 86, 697–705. 10.1016/j.bios.2016.07.015 [PubMed: 27474967]

Claesson-Welsh L, Dejana E, & McDonald DM (2021). Permeability of the Endothelial Barrier: Identifying and Reconciling Controversies. In Trends in Molecular Medicine (Vol. 27, Issue 4). 10.1016/j.molmed.2020.11.006

Comper WD, & Glasgow EF (1995). Charge selectivity in kidney ultrafiltration. In Kidney International (Vol. 47, Issue 5). 10.1038/ki.1995.178

Cross VL, Zheng Y, Won Choi N, Verbridge SS, Sutermaster BA, Bonassar LJ, Fischbach C, & Stroock AD (2010). Dense type I collagen matrices that support cellular remodeling and microfabrication for studies of tumor angiogenesis and vasculogenesis in vitro. Biomaterials, 31(33), 8596–8607. 10.1016/j.biomaterials.2010.07.072 [PubMed: 20727585]

Cucullo L, Hossain M, Tierney W, & Janigro D (2013). A new dynamic in vitro modular capillaries-venules modular system: Cerebrovascular physiology in a box. BMC Neuroscience, 14(1), 1–12. 10.1186/1471-2202-14-18/FIGURES/5 [PubMed: 23280045]

Dabagh M, Jalali P, Butler PJ, Randles A, & Tarbell JM (2017). Mechanotransmission in endothelial cells subjected to oscillatory and multi-directional shear flow. Journal of the Royal Society Interface, 14(130), 20170185. 10.1098/rsif.2017.0185 [PubMed: 28515328]

Decsi B, Krammer R, Hegedus K, Ender F, Gyarmati B, Szilágyi A, Totos R, Katona G, Paizs C, Balogh GT, Poppe L, & Balogh-Weiser D (2019). Liver-on-a-chip-magnetic nanoparticle bound synthetic metalloporphyrin-catalyzed biomimetic oxidation of a drug in a magnechip reactor. Micromachines, 10(10). 10.3390/mi10100668

Deng X, Zeng T, Li J, Huang C, Yu M, Wang X, Tan L, Zhang M, Li A, & Hu J (2019). Kidney-targeted triptolide-encapsulated mesoscale nanoparticles for high-efficiency treatment of kidney injury. Biomaterials Science, 7(12). 10.1039/c9bm01290g

Deplaine G, Safeukui I, Jeddi F, Lacoste F, Brousse V, Perrot S, Biligui S, Guillotte M, Guitton C, Dokmak S, Aussilhou B, Sauvanet A, Hatem DC, Paye F, Thellier M, Mazier D, Milon G, Mohandas N, Mercereau-Puijalon O, … Buffet PA (2011). The sensing of poorly deformable red blood cells by the human spleen can be mimicked in vitro. Blood, 117(8). 10.1182/blood-2010-10-312801

Dixon LJ, Barnes M, Tang H, Pritchard MT, & Nagy LE (2013). Kupffer Cells in the Liver. Comprehensive Physiology, 3(2), 785. 10.1002/CPHY.C120026 [PubMed: 23720329]

Du B, Yu M, & Zheng J (2018). Transport and interactions of nanoparticles in the kidneys. In Nature Reviews Materials (Vol. 3, Issue 10). 10.1038/s41578-018-0038-3

Edington CD, Chen WLK, Geishecker E, Kassis T, Soenksen LR, Bhushan BM, Freake D, Kirschner J, Maass C, Tsamandouras N, Valdez J, Cook CD, Parent T, Snyder S, Yu J, Suter E, Shockley M, Velazquez J, Velazquez JJ, … Griffith LG (2018). Interconnected Microphysiological Systems for Quantitative Biology and Pharmacology Studies. Scientific Reports, 8(1), 4530. 10.1038/s41598-018-22749-0 [PubMed: 29540740]

Ehsan SM, & George SC (2015). Vessel network formation in response to intermittent hypoxia is frequency dependent. Journal of Bioscience and Bioengineering, 120(3), 347–350. 10.1016/j.jbiosc.2015.01.017 [PubMed: 25735591]

Esch MB, King TL, & Shuler ML (2011). The Role of Body-on-a-Chip Devices in Drug and Toxicity Studies. Annual Review of Biomedical Engineering, 13(1), 55–72. 10.1146/annurev-bioeng-071910-124629

Esch MB, Mahler GJ, Stokol T, & Shuler ML (2014). Body-on-a-chip simulation with gastrointestinal tract and liver tissues suggests that ingested nanoparticles have the potential to cause liver injury. *Lab on a Chip* - Miniaturisation for Chemistry and Biology, 14(16). 10.1039/c4lc00371c

Esch MB, Post DJ, Shuler ML, & Stokol T (2011). Characterization of in vitro endothelial linings grown within microfluidic channels. *Tissue Engineering* - Part A, 17(23–24). 10.1089/ten.tea.2010.0371

Esch MB, Prot JM, Wang YI, Miller P, Llamas-Vidales JR, Naughton BA, Applegate DR, & Shuler ML (2015). Multi-cellular 3D human primary liver cell culture elevates metabolic activity under fluidic flow. Lab on a Chip, 15(10), 2269–2277. 10.1039/c5lc00237k [PubMed: 25857666]

Esch MB, & Shuler ML (2015). Modular cell culture platform with passive fluid controls for GI tract - Liver tissue co-culture. Food, Pharmaceutical and Bioengineering Division 2015 - Core Programming Area at the 2015 AIChE Meeting, 2.

Esch MB, Sung JH, Yang J, Yu C, Yu J, March JC, & Shuler ML (2012). On chip porous polymer membranes for integration of gastrointestinal tract epithelium with microfluidic “body-on-a-chip” devices. Biomedical Microdevices, 14(5). 10.1007/s10544-012-9669-0

Esch MB, Ueno H, Applegate DR, & Shuler ML (2016). Modular, pumpless body-on-a-chip platform for the co-culture of GI tract epithelium and 3D primary liver tissue. Lab on a Chip, 16(14), 2719–2729. 10.1039/C6LC00461J [PubMed: 27332143]

Fathi P, & Esch MB (2022). Fabrication and Use of a Pumpless Microfluidic Lymphatic Vessel Chip. In Methods in Molecular Biology (Vol. 2373, pp. 177–199). 10.1007/978-1-0716-1693-2_11 [PubMed: 34520013]

Fede C, Albertin G, Petrelli L, de Caro R, Fortunati I, Weber V, & Ferrante C (2017). Influence of shear stress and size on viability of endothelial cells exposed to gold nanoparticles. J Nanopart Res, 19(9), 316. 10.1007/s11051-017-3993-5 [PubMed: 28959137]

Fede C, Fortunati I, Weber V, Rossetto N, Bertasi F, Petrelli L, Guidolin D, Signorini R, de Caro R, Albertin G, & Ferrante C (2015). Evaluation of gold nanoparticles toxicity towards human endothelial cells under static and flow conditions. Microvasc Res, 97, 147–155. 10.1016/j.mvr.2014.10.010 [PubMed: 25446009]

Frerking I, Günther A, Seeger W, & Pison U (2001). Pulmonary surfactant: functions, abnormalities and therapeutic options. Intensive Care Medicine, 27(11), 1699–1717. 10.1007/s00134-001-1121-5 [PubMed: 11810113]

Gallardo PA, & Vio CP (2022). Glomerular Filtration and Renal Blood Flow. Renal Physiology and Hydrosaline Metabolism, 29–51. 10.1007/978-3-031-10256-1_3

Graff P, Hönzke S, Joshi AA, Yealland G, Fleige E, Unbehauen M, Schäfer-Korting M, Hocke A, Haag R, & Hedtrich S (2022). Preclinical Testing of Dendritic Core-Multishell Nanoparticles in Inflammatory Skin Equivalents. Molecular Pharmaceutics, 19(6). 10.1021/acs.molpharmaceut.1c00734

Hargrove-Grimes P, Low LA, & Tagle DA (2022). Microphysiological Systems: Stakeholder Challenges to Adoption in Drug Development. In Cells Tissues Organs (Vol. 211, Issue 3). 10.1159/000517422

Herron LA, Hansen CS, & Abaci HE (2019). Engineering tissue-specific blood vessels. Bioengineering & Translational Medicine, 4(3). 10.1002/BTM2.10139

Huang Y, Wang J, Jiang K, & Chung EJ (2021). Improving kidney targeting: The influence of nanoparticle physicochemical properties on kidney interactions. In Journal of Controlled Release (Vol. 334). 10.1016/j.jconrel.2021.04.016

Huh D, Fujioka H, Tung Y-C, Futai N, Paine R, Grotberg JB, & Takayama S (2007). Acoustically detectable cellular-level lung injury induced by fluid mechanical stresses in microfluidic airway systems. Proceedings of the National Academy of Sciences of the United States of America, 104(48), 18886–18891. 10.1073/pnas.0610868104 [PubMed: 18006663]

Huh D, Matthews BD, Mammoto A, Montoya-Zavala M, Hsin HY, & Ingber DE (2010). Reconstituting Organ-Level Lung Functions on a Chip. Science, 328(5986), 1662–1668. 10.1126/science.1188302 [PubMed: 20576885]

Jamieson JJ, Searson PC, & Gerecht S (2017). Engineering the human blood-brain barrier in vitro. Journal of Biological Engineering, 11(1). 10.1186/S13036-017-0076-1

Jeon HM, Kim K, Choi KC, & Sung GY (2020). Side-effect test of sorafenib using 3-D skin equivalent based on microfluidic skin-on-a-chip. Journal of Industrial and Engineering Chemistry, 82, 71–80. 10.1016/j.jiec.2019.09.044

Jeon J. won, Lee SH, Kim D, & Sung JH (2021). In vitro hepatic steatosis model based on gut–liver-on-a-chip. Biotechnology Progress, 37(3). 10.1002/btpr.3121

Jiang T, Guo H, Xia YN, Liu Y, Chen D, Pang G, Feng Y, Yu H, Wu Y, Zhang S, Wang Y, Wang Y, Wen H, & Zhang LW (2021). Hepatotoxicity of copper sulfide nanoparticles towards hepatocyte spheroids using a novel multi-concave agarose chip method. Nanomedicine, 16(17). 10.2217/nnm-2021-0011

Kang JH, Super M, Yung CW, Cooper RM, Domansky K, Graveline AR, Mammoto T, Berthet JB, Tobin H, Cartwright MJ, Watters AL, Rottman M, Waterhouse A, Mammoto A, Gamini N, Rodas MJ, Kole A, Jiang A, Valentin TM, … Ingber DE (2014). An extracorporeal blood-cleansing device for sepsis therapy. Nature Medicine, 20(10). 10.1038/nm.3640

Kang YBA, Eo J, Mert S, Yarmush ML, & Usta OB (2018). Metabolic Patterning on a Chip: Towards in vitro Liver Zonation of Primary Rat and Human Hepatocytes. Scientific Reports, 8(1). 10.1038/s41598-018-27179-6

Kang YBA, Sodunke TR, Lamontagne J, Cirillo J, Rajiv C, Bouchard MJ, & Noh M (2015). Liver sinusoid on a chip: Long-term layered co-culture of primary rat hepatocytes and endothelial cells in microfluidic platforms. Biotechnology and Bioengineering, 112(12), 2571–2582. 10.1002/BIT.25659 [PubMed: 25994312]

Kang YB, Eo J, Bulutoglu B, Yarmush ML, & Usta OB (2020). Progressive hypoxia-on-a-chip: An in vitro oxygen gradient model for capturing the effects of hypoxia on primary hepatocytes in health and disease. Biotechnology and Bioengineering, 117(3). 10.1002/bit.27225

Kim D, Lin YS, & Haynes CL (2011). On-chip evaluation of shear stress effect on cytotoxicity of mesoporous silica nanoparticles. Anal Chem, 83(22), 8377–8382. 10.1021/ac202115a [PubMed: 22032307]

Kim K, Jeon HM, Choi KC, & Sung GY (2020). Testing the effectiveness of curcuma longa leaf extract on a skin equivalent using a pumpless skin-on-a-chip model. International Journal of Molecular Sciences, 21(11), 1–15. 10.3390/ijms21113898

Kim S, Lee H, Chung M, & Jeon NL (2013). Engineering of functional, perfusable 3D microvascular networks on a chip. Lab on a Chip, 13(8), 1489–1500. 10.1039/c3lc41320a [PubMed: 23440068]

LaValley DJ, Miller PG, & Shuler ML (2021). Pumpless, unidirectional microphysiological system for testing metabolism-dependent chemotherapeutic toxicity. Biotechnology Progress, 37(2). 10.1002/btpr.3105

Lee H, Kim DS, Ha SK, Choi I, Lee JM, & Sung JH (2017). A pumpless multi-organ-on-a-chip (MOC) combined with a pharmacokinetic-pharmacodynamic (PK-PD) model. Biotechnology and Bioengineering, 114(2), 432–443. 10.1002/bit.26087 [PubMed: 27570096]

Lee S, Jin SP, Kim YK, Sung GY, Chung JH, & Sung JH (2017). Construction of 3D multicellular microfluidic chip for an in vitro skin model. Biomedical Microdevices, 19(2). 10.1007/s10544-017-0156-5

Li H, Cheng F, Wang Z, Li W, Antonio J, Ac R-L, & Zhang YS (2022). 3D-printed, configurable, paper-based, and autonomous multi-organ-on-paper platforms †. 10.1039/d2me00142j

Li L, Gokduman K, Gokaltun A, Yarmush ML, & Usta OB (2019). A microfluidic 3D hepatocyte chip for hepatotoxicity testing of nanoparticles. Nanomedicine (Lond), 14(16), 2209–2226. 10.2217/nnm-2019-0086 [PubMed: 31179822]

Li Y, Wu Y, Liu Y, Deng QH, Mak M, & Yang X (2019). Atmospheric nanoparticles affect vascular function using a 3D human vascularized organotypic chip. Nanoscale, 11(33). 10.1039/c9nr03622a

Liu J, Feng C, Zhang M, Song F, & Liu H (2022). Design and Fabrication of a Liver-on-a-chip Reconstructing Tissue-tissue Interfaces. Frontiers in Oncology, 12. 10.3389/fonc.2022.959299

Livingston CA, Fabre KM, & Tagle DA (2016). Facilitating the commercialization and use of organ platforms generated by the microphysiological systems (Tissue Chip) program through public-private partnerships. In *Computational and Structural Biotechnology Journal* (Vol. 14). 10.1016/j.csbj.2016.04.003

Lu RXZ, Lai BFL, Benge T, Wang EY, Davenport Huyer L, Rafatian N, & Radisic M (2021). Heart-on-a-Chip Platform for Assessing Toxicity of Air Pollution Related Nanoparticles. Advanced Materials Technologies, 6(2). 10.1002/admt.202000726

MacParland SA, Tsoi KM, Ouyang B, Ma XZ, Manuel J, Fawaz A, Ostrowski MA, Alman BA, Zilman A, Chan WCW, & McGilvray ID (2017). Phenotype Determines Nanoparticle Uptake by Human Macrophages from Liver and Blood. ACS Nano, 11(3). 10.1021/acsnano.6b06245

Maharjan S, Cecen B, & Zhang YS (2020). 2000235 (1 of 21) 3D Immunocompetent Organ-on-a-Chip Models. 10.1002/smtd.202000235

Mahler GJ, Esch MB, Glahn RP, & Shuler ML (2009). Characterization of a gastrointestinal tract microscale cell culture analog used to predict drug toxicity. Biotechnology and Bioengineering, 104(1). 10.1002/bit.22366

Mahler GJ, Esch MB, Tako E, Southard TL, Archer SD, Glahn RP, & Shuler ML (2012). Oral exposure to polystyrene nanoparticles affects iron absorption. Nature Nanotechnology, 7(4). 10.1038/nnano.2012.3

Mahler GJ, & Zhang S (2021). Microfluidic modeling of the glomerulus and tubular appartus. In Regenerative Nephrology. 10.1016/B978-0-12-823318-4.00021-4

Malik M, Yang Y, Fathi P, Mahler GJ, & Esch MB (2021). Critical Considerations for the Design of Multi-Organ Microphysiological Systems (MPS). In *Frontiers in Cell and Developmental Biology* (Vol. 9). 10.3389/fcell.2021.721338

Marieb EN, & Hoehn K (2019). Human Anantomy & Physiology.

Miller PG, & Shuler ML (2016). Design and demonstration of a pumpless 14 compartment microphysiological system. Biotechnology and Bioengineering, 113(10), 2213–2227. 10.1002/bit.25989 [PubMed: 27070809]

Moghimi SM, Hunter AC, & Murray JC (2001). Long-circulating and target-specific nanoparticles: Theory to practice. In Pharmacological Reviews (Vol. 53, Issue 2).

Moradi E, Jalili-Firoozinezhad S, & Solati-Hashjin M (2020). Microfluidic organ-on-a-chip models of human liver tissue. In *Acta Biomaterialia* (Vol. 116). 10.1016/j.actbio.2020.08.041

Moya M, Tran D, & George SC (2013). An integrated in vitro model of perfused tumor and cardiac tissue. In *Stem Cell Research and Therapy* (Vol. 4, Issue SUPPL.1). 10.1186/scrt376

Musah S, Mammoto A, Ferrante TC, Jeanty SSF, Hirano-Kobayashi M, Mammoto T, Roberts K, Chung S, Novak R, Ingram M, Fatanat-Didar T, Koshy S, Weaver JC, Church GM, & Ingber DE (2017). Mature induced-pluripotent-stem-cell-derived human podocytes reconstitute kidney glomerular-capillary-wall function on a chip. Nature Biomedical Engineering, 1(5). 10.1038/s41551-017-0069

Oleaga C, Bernabini C, Smith AST, Srinivasan B, Jackson M, McLamb W, Platt V, Bridges R, Cai Y, Santhanam N, Berry B, Najjar S, Akanda N, Guo X, Martin C, Ekman G, Esch MB, Langer J, Ouedraogo G, … Hickman JJ (2016). Multi-Organ toxicity demonstration in a functional human in vitro system composed of four organs. Scientific Reports, 6. 10.1038/srep20030

Papademetriou I, Vedula E, Charest J, & Porter T (2018). Effect of flow on targeting and penetration of angiopep-decorated nanoparticles in a microfluidic model blood-brain barrier. PLoS One, 13(10), e0205158. 10.1371/journal.pone.0205158 [PubMed: 30300391]

Park TE, Mustafaoglu N, Herland A, Hasselkus R, Mannix R, FitzGerald EA, Prantil-Baun R, Watters A, Henry O, Benz M, Sanchez H, McCrea HJ, Goumnerova LC, Song HW, Palecek SP, Shusta E, & Ingber DE (2019). Hypoxia-enhanced Blood-Brain Barrier Chip recapitulates human barrier function and shuttling of drugs and antibodies. Nat Commun, 10(1), 2621. 10.1038/s41467-019-10588-0 [PubMed: 31197168]

Patil P, Kumeria T, Dusan Losic bc, & Kurkuri M. (2015). Isolation of circulating tumour cells by physical means in a microfluidic device: a review. 10.1039/c5ra16489c

Petrosyan A, Cravedi P, Villani V, Angeletti A, Manrique J, Renieri A, de Filippo RE, Perin L, & da Sacco S (2019). A glomerulus-on-a-chip to recapitulate the human glomerular filtration barrier. Nature Communications, 10(1). 10.1038/s41467-019-11577-z

Picot J, Ndour PA, Lefevre SD, el Nemer W, Tawfik H, Galimand J, da Costa L, Ribeil JA, de Montalembert M, Brousse V, le Pioufle B, Buffet P, le Van Kim C, & Français O (2015). A biomimetic microfluidic chip to study the circulation and mechanical retention of red blood cells in the spleen. American Journal of Hematology, 90(4). 10.1002/ajh.23941

Polidoro MA, Ferrari E, Marzorati S, Lleo A, & Rasponi M (2021). Experimental liver models: From cell culture techniques to microfluidic organs-on-chip. Liver International, 41(8), 1744–1761. 10.1111/LIV.14942 [PubMed: 33966344]

Ponmozhi J, Dhinakaran S, Varga-medveczky Z, Fónagy K, Bors LA, Iván K, & Erdő F (2021). Development of skin-on-a-chip platforms for different utilizations: Factors to be considered. In Micromachines (Vol. 12, Issue 3, pp. 1–25). 10.3390/mi12030294

Poon W, Zhang YN, Ouyang B, Kingston BR, Wu JLY, Wilhelm S, & Chan WCW (2019). Elimination Pathways of Nanoparticles. ACS Nano, 13(5). 10.1021/acsnano.9b01383

Prot J-M, Bunescu A, Elena-Herrmann B, Aninat C, Snouber LC, Griscom L, Razan F, Bois FY, Legallais C, Brochot C, Corlu A, Dumas ME, & Leclerc E (2012). Predictive toxicology using systemic biology and liver microfluidic “on chip” approaches: Application to acetaminophen injury. Toxicology and Applied Pharmacology, 259(3), 270–280. 10.1016/j.taap.2011.12.017 [PubMed: 22230336]

Rennert K, Steinborn S, Gröger M, Ungerböck B, Jank AM, Ehgartner J, Nietzsche S, Dinger J, Kiehntopf M, Funke H, Peters FT, Lupp A, Gärtner C, Mayr T, Bauer M, Huber O, & Mosig AS (2015). A microfluidically perfused three dimensional human liver model. Biomaterials, 71. 10.1016/j.biomaterials.2015.08.043

Rigat-Brugarolas LG, Elizalde-Torrent A, Bernabeu M, de Niz M, Martin-Jaular L, Fernandez-Becerra C, Homs-Corbera A, Samitier J, & del Portillo HA (2014). A functional microengineered model of the human splenon-on-a-chip. Lab on a Chip, 14(10). 10.1039/c3lc51449h

Risueño I, Valencia L, Jorcano JL, & Velasco D (2021). Skin-on-a-chip models: General overview and future perspectives. In APL Bioengineering (Vol. 5, Issue 3). 10.1063/5.0046376

Ronaldson-Bouchard K, Teles D, Yeager K, Tavakol DN, Zhao Y, Chramiec A, Tagore S, Summers M, Stylianos S, Tamargo M, Lee BM, Halligan SP, Abaci EH, Guo Z, Jacków J, Pappalardo A, Shih J, Soni RK, Sonar S, … Vunjak-Novakovic G (2022). A multi-organ chip with matured tissue niches linked by vascular flow. Nature Biomedical Engineering 2022 6:4, 6(4), 351–371. 10.1038/s41551-022-00882-6

Sakolish CM, & Mahler GJ (2017). A novel microfluidic device to model the human proximal tubule and glomerulus. RSC Advances, 7(8). 10.1039/c6ra25641d

Sakolish CM, Philip B, & Mahler GJ (2019). A human proximal tubule-on-a-chip to study renal disease and toxicity. Biomicrofluidics, 13(1). 10.1063/1.5083138

Samuel SP, Jain N, O’Dowd F, Paul T, Kashanin D, Gerard VA, Gun’ko YK, Prina-Mello A, & Volkov Y (2012). Multifactorial determinants that govern nanoparticle uptake by human endothelial cells under flow. Int J Nanomedicine, 7, 2943–2956. 10.2147/IJN.S30624 [PubMed: 22745555]

Sanches PL, Geaquinto LRDO, Cruz R, Schuck DC, Lorencini M, Granjeiro JM, & Ribeiro ARL (2020). Toxicity evaluation of tio2 nanoparticles on the 3d skin model: A systematic review. Frontiers in Bioengineering and Biotechnology, 8. 10.3389/fbioe.2020.00575

Shah P, Fritz J. v., Glaab E, Desai MS, Greenhalgh K, Frachet A, Niegowska M, Estes M, Jäger C, Seguin-Devaux C, Zenhausern F, & Wilmes P (2016). A microfluidics-based in vitro model of the gastrointestinal human-microbe interface. Nature Communications, 7. 10.1038/ncomms11535

Shinha K, Nihei W, Nakamura H, Goto T, Kawanishi T, Ishida N, Yamazaki N, Imakura Y, Mima S, Inamura K, Arakawa H, Nishikawa M, Kato Y, Sakai Y, & Kimura H (2021). A kinetic pump integrated microfluidic plate (Kim-plate) with high usability for cell culture-based multiorgan microphysiological systems. Micromachines, 12(9). 10.3390/mi12091007

Sin A, Chin KC, Jamil MF, Kostov Y, Rao G, & Shuler ML (2008). The Design and Fabrication of Three-Chamber Microscale Cell Culture Analog Devices with Integrated Dissolved Oxygen Sensors. Biotechnology Progress, 20(1), 338–345. 10.1021/bp034077d

Singh G, & Katyal SL (1997). Clara Cells and Clara Cell 10 kD Protein (CC10). In American Journal of Respiratory Cell and Molecular Biology (Vol. 17, Issue 2, pp. 141–143). 10.1165/ajrcmb.17.2.f138 [PubMed: 9271300]

Smith AS, Long CJ, Berry BJ, McAleer C, Stancescu M, Molnar P, Miller PG, Esch MB, Prot J-M, Hickman JJ, & Shuler ML (2013). Microphysiological systems and low-cost microfluidic platform with analytics. Stem Cell Research and Therapy, 4(SUPPL.1). 10.1186/scrt370

Smith VM, Nguyen H, Rumsey JW, Long CJ, Shuler ML, & Hickman JJ (2021). A Functional Human-on-a-Chip Autoimmune Disease Model of Myasthenia Gravis for Development of Therapeutics. Frontiers in Cell and Developmental Biology, 9. 10.3389/fcell.2021.745897

Song HJ, Lim HY, Chun W, Choi KC, Lee T. yong, Sung JH, & Sung GY (2018). Development of 3D skin-equivalent in a pump-less microfluidic chip. Journal of Industrial and Engineering Chemistry, 60, 355–359. 10.1016/j.jiec.2017.11.022

Song HJ, Lim HY, Chun W, Choi KC, Sung JH, & Sung GY (2017). Fabrication of a pumpless, microfluidic skin chip from different collagen sources. Journal of Industrial and Engineering Chemistry, 56, 375–381. 10.1016/j.jiec.2017.07.034

Song JW, Bazou D, & Munn LL (2012). Anastomosis of endothelial sprouts forms new vessels in a tissue analogue of angiogenesis. Integrative Biology (United Kingdom), 4(8), 857–862. 10.1039/c2ib20061a

Starokozhko V, & Groothuis GMM (2017). Judging the value of 'liver-on-a-chip' devices for prediction of toxicity. In *Expert Opinion on Drug Metabolism and Toxicology* (Vol. 13, Issue 2). 10.1080/17425255.2017.1246537

Stojic M, López V, Montero A, Quílez C, de Aranda Izuzquiza G, Vojtova L, Luis Jorcano J, & Velasco D (2019). Skin tissue engineering. In *Biomaterials for Skin Repair and Regeneration* (pp. 59–99). 10.1016/B978-0-08-102546-8.00003-0

Sung JH, Esch MB, & Shuler ML (2010). Integration of in silico and in vitro platforms for pharmacokineticpharmacodynamic modeling. Expert Opinion on Drug Metabolism and Toxicology, 6(9). 10.1517/17425255.2010.496251

Sung JH, Kam C, & Shuler ML (2010). A microfluidic device for a pharmacokinetic–pharmacodynamic (PK–PD) model on a chip. Lab on a Chip, 10(4), 446. 10.1039/b917763a [PubMed: 20126684]

Sung JH, Wang Y, & Shuler ML (2020). Strategies for using mathematical modeling approaches to design and interpret multi-organ microphysiological systems (MPS). In APL Bioengineering (Vol. 3, Issue 2). 10.1063/1.5097675

Sung JH, Yu J, Luo D, Shuler ML, & March JC (2011). Microscale 3-D hydrogel scaffold for biomimetic gastrointestinal (GI) tract model. Lab Chip, 11(3), 389–392. 10.1039/c0lc00273a [PubMed: 21157619]

Tang S, Peng C, Xu J, Du B, Wang Q, Vinluan RD, Yu M, Kim MJ, & Zheng J (2016). Tailoring Renal Clearance and Tumor Targeting of Ultrasmall Metal Nanoparticles with Particle Density. Angewandte Chemie - International Edition, 55(52). 10.1002/anie.201609043

Tencer J, Frick IM, Öquist BW, Alm P, & Rippe B (1998). Size-selectivity of the glomerular barrier to high molecular weight proteins: Upper size limitations of shunt pathways. Kidney International, 53(3). 10.1046/j.1523-1755.1998.00797.x

Traore MA, & George SC (2017). Tissue Engineering the Vascular Tree. Tissue Engineering Part B: Reviews, 23(6), 505–514. 10.1089/ten.teb.2017.0010 [PubMed: 28799844]

Tronolone JJ, Lam J, Agrawal A, & Sung K (2021). Pumpless, modular, microphysiological systems enabling tunable perfusion for long-term cultivation of endothelialized lumens. Biomedical Microdevices, 23(2). 10.1007/s10544-021-00562-3

van Duinen V, van den Heuvel A, Trietsch SJ, Lanz HL, van Gils JM, van Zonneveld AJ, Vulto P, & Hankemeier T (2017). 96 perfusable blood vessels to study vascular permeability in vitro. Scientific Reports, 7(1). 10.1038/s41598-017-14716-y

Viravaidya K, Sin A, & Shuler ML (2008). Development of a Microscale Cell Culture Analog To Probe Naphthalene Toxicity. Biotechnology Progress, 20(1), 316–323. 10.1021/bp0341996

Vunjak-Novakovic G, Bhatia S, Chen C, & Hirschi K (2013). HeLiVa platform: integrated heart-liver-vascular systems for drug testing in human health and disease. Stem Cell Research & Therapy, 4(Suppl 1), S8. 10.1186/scrt369 [PubMed: 24565063]

Wang L, Tao T, Su W, Yu H, Yu Y, & Qin J (2017). A disease model of diabetic nephropathy in a glomerulus-on-a-chip microdevice. Lab on a Chip, 17(10). 10.1039/c7lc00134g

Wang YI, Abaci HE, & Shuler ML (2017). Microfluidic blood–brain barrier model provides in vivo-like barrier properties for drug permeability screening. Biotechnology and Bioengineering, 114(1), 184–194. 10.1002/bit.26045 [PubMed: 27399645]

Wang YI, Erbil Abaci H, Shuler Nancy E ML, & Bioeng B (2017). Microfluidic Blood-Brain Barrier Model Provides In Vivo-Like Barrier Properties for Drug Permeability Screening Graphical abstract HHS Public Access Author manuscript. Biotechnol Bioeng, 114(1), 184–194. 10.1002/bit.26045. [PubMed: 27399645]

Wang YI, & Shuler ML (2018). UniChip enables long-term recirculating unidirectional perfusion with gravity-driven flow for microphysiological systems. Lab on a Chip, 18(17), 2563–2574. 10.1039/C8LC00394G [PubMed: 30046784]

Wills JW, Hondow N, Thomas AD, Chapman KE, Fish D, Maffeis TG, Penny MW, Brown RA, Jenkins GJS, Brown AP, White PA, & Doak SH (2016). Genetic toxicity assessment of engineered nanoparticles using a 3D in vitro skin model (EpiDerm™). Particle and Fibre Toxicology, 13(1). 10.1186/s12989-016-0161-5

Wufuer M, Lee GH, Hur W, Jeon B, Kim BJ, Choi TH, & Lee SH (2016). Skin-on-a-chip model simulating inflammation, edema and drug-based treatment. Scientific Reports, 6. 10.1038/srep37471

Yang X, Li K, Zhang X, Liu C, Guo B, Wen W, & Gao X (2018). Nanofiber membrane supported lung-on-a-chip microdevice for anti-cancer drug testing. Lab on a Chip, 18(3), 486–495. 10.1039/c7lc01224a [PubMed: 29309077]

Yang Y, Fathi P, Holland G, Pan D, Wang NS, & Esch MB (2019). Pumpless microfluidic devices for generating healthy and diseased endothelia. Lab on a Chip, 19(19), 3212–3219. 10.1039/c9lc00446g [PubMed: 31455960]

Yeon JH, Ryu HR, Chung M, Hu QP, & Jeon NL (2012). In vitro formation and characterization of a perfusable three-dimensional tubular capillary network in microfluidic devices. Lab on a Chip, 12(16), 2815–2822. 10.1039/c2lc40131b [PubMed: 22767334]

Yun SH, Cabrera LM, Song JW, Futai N, Tung YC, Smith GD, & Takayama S (2007). Characterization and resolution of evaporation-mediated osmolality shifts that constrain microfluidic cell culture in poly(dimethylsiloxane) devices. Analytical Chemistry, 79(3). 10.1021/ac061990v

Zhang J, Chen Z, Zhang Y, Wang X, Ouyang J, Zhu J, Yan Y, Sun X, Wang F, Li X, Ye H, Sun S, Yu Q, Sun J, Ge J, Li Q, Han Q, Pu Y, & Gu Z (2021). Construction of a high fidelity epidermis-on-a-chip for scalable: In vitro irritation evaluation. Lab on a Chip, 21(19), 3804–3818. 10.1039/d1lc00099c [PubMed: 34581381]

Zhang M, Xu C, Jiang L, & Qin J (2018a). A 3D human lung-on-a-chip model for nanotoxicity testing. Toxicology Research, 7(6), 1048–1060. 10.1039/c8tx00156a [PubMed: 30510678]

Zhang SY, & Mahler GJ (2021). Modelling renal filtration and reabsorption processes in a human glomerulus and proximal tubule microphysiological system. Micromachines, 12(8). 10.3390/mi12080983

Zhang SY, & Mahler GJ (2022). A glomerulus and proximal tubule microphysiological system simulating renal filtration, reabsorption, secretion, and toxicity. Lab on a Chip, 23(2). 10.1039/d2lc00887d

Zhang YS, Arneri A, Bersini S, Shin SR, Zhu K, Goli-Malekabadi Z, Aleman J, Colosi C, Busignani F, Dell'Erba V, Bishop C, Shupe T, Demarchi D, Moretti M, Rasponi M, Dokmeci MR, Atala A, & Khademhosseini A (2016). Bioprinting 3D microfibrous scaffolds for engineering endothelialized myocardium and heart-on-a-chip. Biomaterials, 110. 10.1016/j.biomaterials.2016.09.003

Zhang Y, Zheng L, Tuo J, Liu Q, Zhang X, Xu Z, Liu S, & Sui G (2017). Analysis of PM2.5-induced cytotoxicity in human HaCaT cells based on a microfluidic system. Toxicology in Vitro, 43. 10.1016/j.tiv.2017.04.018

Zhou M, Zhang X, Wen X, Wu T, Wang W, Yang M, Wang J, Fang M, Lin B, & Lin H (2016). Development of a Functional Glomerulus at the Organ Level on a Chip to Mimic Hypertensive Nephropathy. Scientific Reports, 6. 10.1038/srep31771

Zhu S, Zhang J, Zhang L, Ma W, Man N, Liu Y, Zhou W, Lin J, Wei P, Jin P, Zhang Y, Hu Y, Gu E, Lu X, Yang Z, Liu X, Bai L, & Wen L (2017). Inhibition of Kupffer Cell Autophagy Abrogates Nanoparticle-Induced Liver Injury. Advanced Healthcare Materials, 6(9). 10.1002/adhm.201601252

Zoio P, Lopes-Ventura S, & Oliva A (2021). Barrier-on-a-chip with a modular architecture and integrated sensors for real-time measurement of biological barrier function. Micromachines, 12(7). 10.3390/mi12070816

**Info box 1**

**Pumpless MPS Features**

**Advantages:**

- Pumpless MPS can recirculate small amounts of cell culture medium, making it possible to reduce the liquid levels in the system to near-physiological amounts.
- The systems don't require expensive components like external pumps or integrated microfluidic pumps.

**Disadvantages:**

- In bidirectional flow systems where medium flows back and forth, there must be sufficient medium in the system so that there is no portion of liquid in the channel that becomes nutrient-depleted over time.
- Pumpless systems require to be in motion every 30 s to 60 s (because they are rocked back and forth on a rocker platform or rotated on a rotating platform) and this makes it challenging to integrate them with wired components used for measurements.
- Pumpless systems are typically open to the environment and thereby subject to medium evaporation.

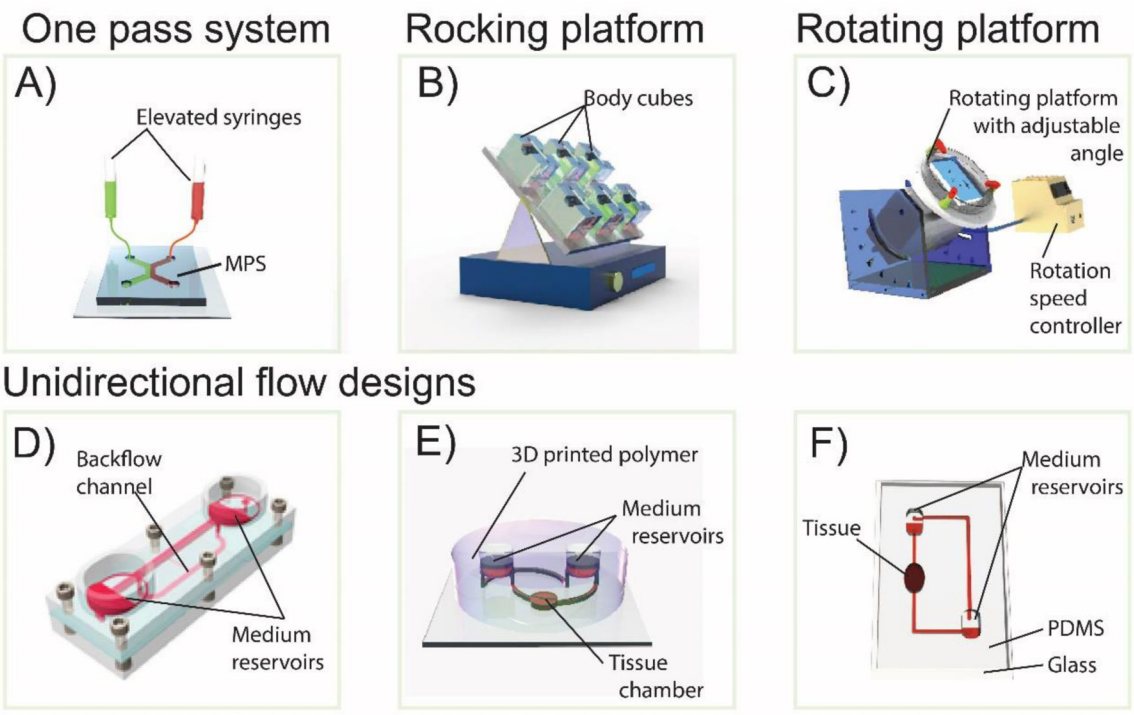


**Fig.1:**

Pumpless MPS - Modes of operation (A) One-pass systems (H. Li et al., 2022), (B) Rocker platform, (C) rotating platform, and unidirectional designs (D) UniChip (reprinted with permission from LOC) (Y. I. Wang & Shuler, 2018), (E) GI-tract – liver system (Esch & Shuler, 2015), and (F) vasculature chip (Y. Yang et al., 2019).

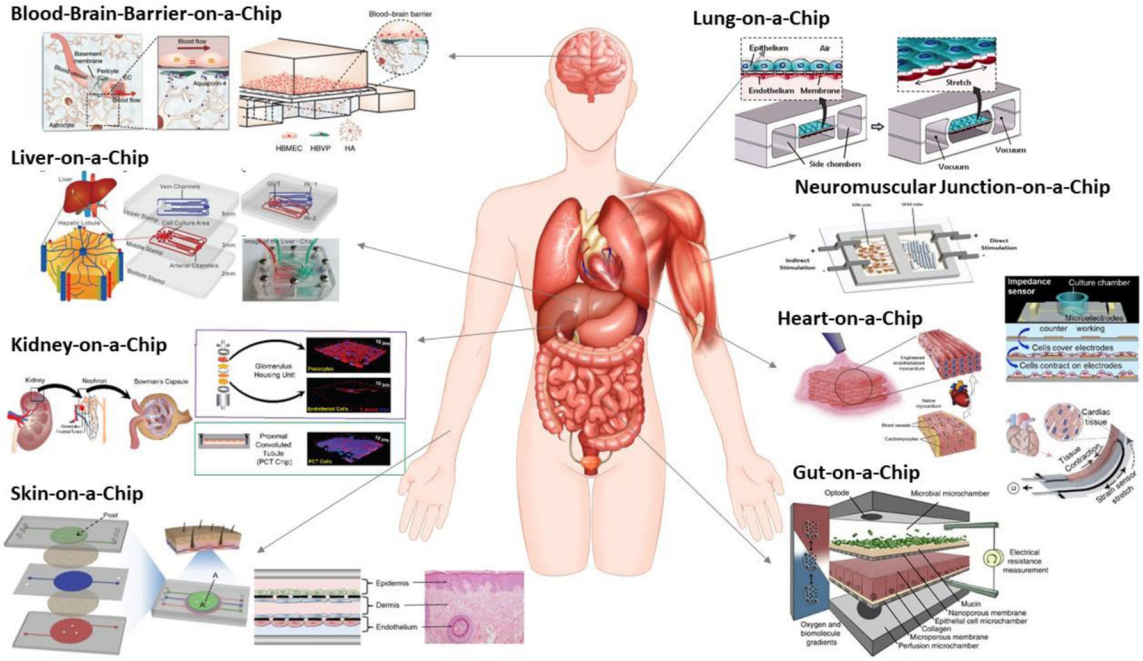


**Fig. 2:**

Examples of microphysiological systems (MPS) of various organs, including Blood-Brain Barrier-in-a-Chip, reprinted from (S. I. Ahn et al., 2020), Liver-on-a-Chip (Liu et al., 2022), Kidney-on-a-Chip with glomerulus and proximal tubules (S. Y. Zhang & Mahler, 2021), Skin-on-a-Chip (Wufuer et al., 2016), Lung-on-a-Chip (Huh et al., 2010) (reprinted with permission from The American Association of Science), Neuromuscular junction-on-a-Chip (V. M. Smith et al., 2021), Heart-on-a-Chip (K. W. Cho et al., 2020; Y. S. Zhang et al., 2016) (reprinted with permission from Elsevier), Gut-on-a-Chip (Shah et al., 2016).

**TABLE 1:**

Examples of pumped and pumpless MPS used to evaluate the impact of nanoparticles on tissues.

| MPS system | Organ-on-a-chip | Cell source | Nanoparticles | Characteristic | References |
|---|---|---|---|---|---|
| Pumped MPS | Blood-Brain-Barrier | bEnd.3 BMVEC | Angiopep-2 conjugated liposomes/quantum dots (QDs) | Nanoparticle penetration | (Papademetriou et al., 2018; Park et al., 2019; Y. I. Wang, Abaci, et al., 2017) |
| | Liver | Rat hepatocyte | Fe3O4 nanoparticle CuS nanoparticles | Nanoparticle toxicity | (Jiang et al., 2021; L. Li et al., 2019) |
| | Liver/Gut | Caco-2/HT29-MTX with HepG2/C3A cells | Carboxylated polystyrene (PS) | Nanoparticle toxicity: elimination | (Esch et al., 2014) |
| | Lung | HUVECs HPAEpiC | ZnO, $TiO_2$ Silica nanoparticle | Nanoparticle toxicity, penetration | (Huh et al., 2010; X. Yang et al., 2018; M. Zhang et al., 2018) |
| | Heart | NRVMs HUVECs iPSC-derived cadiomyocytes | $TiO_2$, Ag nanoparticle CuO, $SiO_2$ | Nanoparticle toxicity | (S. Ahn et al., 2018; Lu et al., 2021) |
| | Spleen | RBCs | Magnetic nanobeads | Nanoparticle elimination | (J. H. Kang et al., 2014) |
| | Kidney | Renal adenocarcinoma cells | Carboxylated polystyrene (PS) | Toxicity | (S. Cho et al., 2016) |
| | Vascular | HUVECs | Au nanoparticle QDs, $SiO_2$ nanoparticle | Nanoparticle toxicity, uptake | (Y. Y. Chen et al., 2020; Fede et al., 2015, 2017; D. Kim et al., 2011; Y. Li et al., 2019; Samuel et al., 2012)(Y. Y. Chen et al., 2020; Fede et al., 2015, 2017; D. Kim et al., 2011; Y. Li et al., 2019; Samuel et al., 2012) |
| Pumpless MPS | Liver | HepG2/C3A | | Drug toxicity | (Sung, Kam, et al., 2010) |
| | Liver/Gut | Caco-2/HT29-MTX with HepG2/C3A cells | Carboxylated polystyrene (PS), Turofexorate isopropyl (XL-335), metformin | Nanoparticle toxicity: elimination | (H. J. Chen et al., 2018; Esch & Shuler, 2015; J. won Jeon et al., 2021) |
| | 3D GI tract | Colon carcinoma cell line, Caco-2 cells, epithelial cells | | | (Sung et al., 2011) |
| | Skin | HSE from fibroblasts and keratinocytes | NA | Drug toxicity | (Abaci et al., 2015; H. M. Jeon et al., 2020; H. J. Song et al., 2018) |
| | Body | A549 (lung), Caco2 (GI), HepG2 C3A (liver), Meg01 (bone marrow), HK2 (kidney) | NA | Drug distribution | (L. Chen et al., 2020; LaValley et al., 2021; H. Li et al., 2022; Miller & Shuler, 2016) |

*Abbreviations:* HUVECs, Human umbilical vein endothelial cells; HPAEpiC, Human alveolar epithelial cells; Caco-2/HT29-MTX; HepG2/C3A; Caco-2BBE; bEnd.3, Brain microvascular endothelial cells; BMVEC, iPSC-derived brain-like microvascular endothelial cells; RBCs, red blood cells; HSE, human skin equivalents; NRVMs, Neonatal rat ventricular myocytes; NA, not applicable.